Progress In Electromagnetics Research, Vol. 141, 751–768, 2013

ORBITAL ANGULAR MOMENTUM DENSITY OF AN ELEGANT LAGUERRE-GAUSSIAN BEAM

Guoquan Zhou[1, *] and Guoyun Ru[2]

[1]School of Sciences, Zhejiang A & F University, Lin'an 311300, China

[2]ASML Inc., 77 Danbury Road, Wilton, CT 06897, USA

Abstract—Based on the method of the vectorial angular spectrum, an analytical expression of the electric field of an elegant Laguerre-Gaussian beam in free space is derived beyond the paraxial approximation, and the corresponding magnetic field is obtained by taking the curl of the electric field. By using the expressions for the electromagnetic fields, the expression of the orbital angular momentum density of the elegant Laguerre-Gaussian beam is derived, which is applicable to both the near and far fields. The effects of the three beam parameters on the distribution of the orbital angular momentum density of the elegant Laguerre-Gaussian beam are studied. The distribution of the orbital angular momentum density of the elegant Laguerre-Gaussian beam is also compared with that of the standard Laguerre-Gaussian beam. The result shows that the distribution of the orbital angular momentum density of the elegant Laguerre-Gaussian beam is more simple and centralized than that of the standard Laguerre-Gaussian beam.

1. INTRODUCTION

The higher-order modes of axially symmetric laser cavities with spherical mirrors are the standard Laguerre-Gaussian beams. As an extension of the standard Laguerre-Gaussian beams, an elegant Laguerre-Gaussian beam has been introduced [1]. The elegant Laguerre-Gaussian beams are also the eigenmodes of the paraxial wave equation. In the expression of the standard Laguerre-Gaussian beams where the paraxial approximation is applied, only the Gaussian part has a complex argument. While in the expression of the elegant Laguerre-Gaussian beams where the paraxial approximation holds,

Received 16 May 2013, Accepted 6 July 2013, Scheduled 12 August 2013

* Corresponding author: Guoquan Zhou (zhouguoquan178@sohu.com).

the arguments are both complex in the Gaussian and the Laguerre parts [1]. The properties of the elegant Laguerre-Gaussian beams propagating in free space [2–4], through a paraxial $ABCD$ optical system [5], in apertured fractional Hankel transform systems [6], through aligned and misaligned paraxial optical systems [7], at a dielectric interface [8], in turbulent atmosphere [9], in non-Kolmogorov turbulence [10], by an opaque obstacle [11], and in a uniaxial crystal [12] have been extensively investigated. Based on the expansion of the hard aperture function into a finite sum of complex Gaussian functions, the propagation characteristics of truncated elegant Laguerre-Gaussian beams have been examined [13, 14]. The vectorial structure of the elegant Laguerre-Gaussian beam has been depicted in the far-field regime [15]. Higher-order complex source has been proposed to generate the elegant Laguerre-Gaussian beams [16]. The relationship between the elegant Laguerre-Gaussian and the Bessel-Gaussian beams has been revealed [17]. Diagonal relations between elegant Hermite-Gaussian and Laguerre-Gaussian beams have also been evaluated [18]. New fractional-order solutions, which smoothly connect the elegant Laguerre-Gaussian beams of integral-order, of the paraxial wave equation have been presented by means of the tools of fractional calculus [19]. Elegant Laguerre-Gaussian beams can be used as a new tool to describe the axisymmetric flattened Gaussian beam [20]. The elegant Laguerre-Gaussian beams have also been extended to the nonparaxial case [21, 22] and the partially coherent case [23–25].

Elegant Laguerre-Gaussian beams carry the orbital angular momentum and can impart this angular momentum to microscopic particles. Therefore, the elegant Laguerre-Gaussian beam can be applied to optical trapping, optical micro-manipulation, nonlinear optics, and quantum information processing [26–32]. To our best knowledge, however, the research in the orbital angular momentum density of the elegant Laguerre-Gaussian beam has not been reported so far. In the remainder of this paper, therefore, we investigate the orbital angular momentum density of the elegant Laguerre-Gaussian beam. Moreover, we treat the elegant Laguerre-Gaussian beam beyond the paraxial approximation. Under the condition of the paraxial approximation, the elegant Laguerre-Gaussian beam is described by the solution of the paraxial wave equation. When extended to the case beyond the paraxial approximation, the perturbation method in the scalar theory, the Lommel's lemma in the vectorial theory, and the vectorial Rayleigh-Sommerfeld formulae are usually used to describe the elegant Laguerre-Gaussian beam. Here the description of the elegant Laguerre-Gaussian beam is based on the method of the vectorial angular spectrum. By using the electromagnetic fields of the elegant Laguerre-Gaussian beam beyond the paraxial approximation, the expression of the orbital angular momentum density of the elegant Laguerre-Gaussian beam is derived in free space. As the overall transverse component of the orbital angular momentum is zero, only the longitudinal component of the orbital angular momentum density is considered. The effects of the beam parameters on the distribution of the orbital angular momentum density of the elegant Laguerre-Gaussian beam are also discussed.

2. ORBITAL ANGULAR MOMENTUM DENSITY OF AN ELEGANT LAGURRE-GAUSSIAN BEAM

The z-axis is taken to be the propagation axis. The elegant Laguerre-Gaussian beam is assumed to be linearly polarized along the x-direction, and the y-component of the optical field is equal to zero. The elegant Laguerre-Gaussian beam in the source plane $z = 0$ takes the form of

$$E_x(\rho, 0, \theta) = \left(\frac{\rho}{w_0}\right)^m L_n^m \left(\frac{\rho^2}{w_0^2}\right) \exp\left(-\frac{\rho^2}{w_0^2}\right) \exp(im\theta), \tag{1}$$

where w_0 is the beam waist width of the fundamental Gaussian mode, and L_n^m is the associated Laguerre polynomial. n and m are the radial and angular mode numbers, respectively. $\rho = (x^2 + y^2)^{1/2}$ and $\theta = \tan^{-1}(y/x)$. The time dependent factor $\exp(-i\omega t)$ is omitted in Eq. (1), and ω is the angular frequency. Due to the radial and azimuthal symmetry, the method of the vectorial angular spectrum is used to derive the propagating electromagnetic fields of the elegant Laguerre-Gaussian beam, which will result in the relatively simple formulae. The exact description of the elegant Laguerre-Gaussian beam should be directly initiated from Maxwell's equations. Moreover, the method of the vectorial angular spectrum is a useful tool to resolve Maxwell's equations. Eq. (1) is the boundary condition of Maxwell's equations. The elegant Laguerre-Gaussian beam should satisfy the Maxwell's equations:

$$\nabla \times \mathbf{E}(\rho, z, \theta) - ik\mathbf{H}(\rho, z, \theta) = 0, \tag{2}$$

$$\nabla \times \mathbf{H}(\rho, z, \theta) + ik\mathbf{E}(\rho, z, \theta) = 0, \tag{3}$$

$$\nabla \cdot \mathbf{E}(\rho, z, \theta) = \nabla \cdot \mathbf{H}(\rho, z, \theta) = 0, \tag{4}$$

where $k = 2\pi/\lambda$ is the wave number with λ being the optical wavelength. $\mathbf{E}(\rho, z, \theta)$ and $\mathbf{H}(\rho, z, \theta)$ are the propagating electromagnetic fields. When the Maxwell's equations are transformed from the space domain into the frequency domain, Eqs. (2)–(4) become

$$\mathbf{L}\times\tilde{\mathbf{E}}(p,q,z)-ik\tilde{\mathbf{H}}(p,q,z) = 0, \tag{5}$$

$$\mathbf{L}\times\tilde{\mathbf{H}}(p,q,z)+ik\tilde{\mathbf{E}}(p,q,z) = 0, \tag{6}$$

$$\mathbf{L}\cdot\tilde{\mathbf{E}}(p,q,z)=\mathbf{L}\cdot\tilde{\mathbf{H}}(p,q,z) = 0, \tag{7}$$

where $\mathbf{L}=ikp\mathbf{i}+ikq\mathbf{j}+\partial/\partial z\mathbf{k}$. $\mathbf{i}$, $\mathbf{j}$, and $\mathbf{k}$ are the unit vectors in the x-, y-, and z-directions, respectively. p/λ and q/λ are the transverse frequencies. $\tilde{\mathbf{E}}(p,q,z)$ and $\mathbf{E}(\rho,z,\theta)$ are the spatial Fourier transform pair:

$$\mathbf{E}(\rho,z,\theta)=\int_{-\infty}^{\infty}\int_{-\infty}^{\infty}\tilde{\mathbf{E}}(p,q,z)\exp[ik(px+qy)]dpdq. \tag{8}$$

$\tilde{\mathbf{H}}(p,q,z)$ and $\mathbf{H}(\rho,z,\theta)$ are also the spatial Fourier transform pair:

$$\mathbf{H}(\rho,z,\theta)=\int_{-\infty}^{\infty}\int_{-\infty}^{\infty}\tilde{\mathbf{H}}(p,q,z)\exp[ik(px+qy)]dpdq. \tag{9}$$

The solutions of Eqs. (5)–(7) can be expressed in the form as

$$\tilde{\mathbf{E}}(p,q,z) = \mathbf{A}(p,q)\exp(ik\gamma z), \tag{10}$$

$$\tilde{\mathbf{H}}(p,q,z) = \sqrt{\frac{\varepsilon_0}{\mu_0}}[\mathbf{s}\times\mathbf{A}(p,q)]\exp(ik\gamma z), \tag{11}$$

where $\mathbf{A}(p,q)$ is the vector angular spectrum. $\gamma=(1-p^2-q^2)^{1/2}$, $\mathbf{s}=p\mathbf{i}+q\mathbf{j}+\gamma\mathbf{k}$. ε_0 and μ_0 are the electric permittivity and the magnetic permeability in vacuum, respectively. The vector angular spectrum $\mathbf{A}(p,q)$ reads as

$$\mathbf{A}(p,q)=A_x(p,q)\mathbf{i}+A_y(p,q)\mathbf{j}+A_z(p,q)\mathbf{k}. \tag{12}$$

The transverse components of the vector angular spectrum $A_x(p,q)$ and $A_y(p,q)$ are given by the Fourier transform of of the transversal components of initial electric field. The longitudinal component of the vector angular spectrum $A_z(p,q)$ is given by the orthogonal relation $\mathbf{s}\cdot\mathbf{A}(p,q)=0$ and turns out to be

$$A_z(p,q)=-[pA_x(p,q)+qA_y(p,q)]/\gamma. \tag{13}$$

Therefore, the propagating electric field of the elegant Laguerre-Gaussian beam in the z-plane is found to be

$$\mathbf{E}(\rho,z,\theta) = \int_0^{\infty}\int_0^{2\pi}A_x(b,\varphi)\left(\mathbf{i}-\frac{b\cos\varphi}{\gamma}\mathbf{k}\right)\exp\{ik[b\rho\cos(\varphi-\theta)+\gamma z]\}bdbd\varphi, \tag{14}$$

where $b^2 = (p^2 + q^2)^{1/2}$, and $\varphi = \tan^{-1}(q/p)$. $A_x(b, \varphi)$ is the x component of the vector angular spectrum and is given by the Fourier transformation of the x-component of initial electric field [33]:

$$A_x(b,\varphi) = \frac{1}{\lambda^2}\int_0^\infty\int_0^{2\pi}\left(\frac{\rho'}{w_0}\right)^m L_n^m\left(\frac{\rho'^2}{w_0^2}\right)\exp\left(-\frac{\rho'^2}{w_0^2}\right) \exp\left[im\theta' - ikb\rho'\cos\left(\theta'-\varphi\right)\right]\rho' d\rho' d\theta', \tag{15}$$

We recall the following mathematical formulae [34]:

$$\int_0^{2\pi}\exp\left[im\theta' - ikb\rho'\cos\left(\theta'-\varphi\right)\right]d\theta' = 2\pi(-i)^m J_m(kb\rho')\exp(im\varphi), \tag{16}$$

$$L_n^m\left(\frac{\rho'^2}{w_0^2}\right) = \sum_{l=0}^{n}\frac{(-1)^l}{l!}\begin{pmatrix} n+m \\ n-l \end{pmatrix}\frac{\rho'^{2l}}{w_0^{2l}}, \tag{17}$$

$$\int_0^\infty \frac{\rho'^{2l+m}}{w_0^{2l+m}} J_m(kb\rho')\exp\left(-\frac{\rho'^2}{w_0^2}\right)\rho' d\rho' = \frac{w_0^2 l!}{2}\left(\frac{b}{2f}\right)^m \exp\left(-\frac{b^2}{4f^2}\right) L_l^m\left(\frac{b^2}{4f^2}\right), \tag{18}$$

where J_m is the m-th order Bessel function of the first kind and $f = 1/kw_0$. The x-component of the vector angular spectrum is found to be

$$A_x(b,\varphi) = \frac{(-i)^m}{4\pi f^2}\exp(im\varphi)\sum_{l=0}^{n}(-1)^l\begin{pmatrix} n+m \\ n-l \end{pmatrix}\left(\frac{b}{2f}\right)^m \exp\left(-\frac{b^2}{4f^2}\right) L_l^m\left(\frac{b^2}{4f^2}\right). \tag{19}$$

The x-component of the optical field of the elegant Laguerre-Gaussian beam yields

$$E_x(\rho,z,\theta) = \frac{1}{f^2}\sum_{l=0}^{n}\sum_{s=0}^{l}\frac{(-1)^{l+s}}{2^{2s+m+1}s!}\begin{pmatrix} n+m \\ n-l \end{pmatrix}\begin{pmatrix} l+m \\ l-s \end{pmatrix}\int_0^\infty\frac{b^{2s+m}}{f^{2s+m}} \exp\left(-\frac{b^2}{4f^2}\right) J_m(kb\rho)\exp(im\theta + ik\gamma z) b db. \tag{20}$$

When z is larger than several wavelengths, the effect of the evanescent waves can be ignored. Therefore, the upper limit of integral in Eq. (20) can be replaced by 1. In this case, $\exp(ik\gamma z)$ can be expanded as [34]

$$\exp(ik\gamma z) = \sum_{u=0}^{\infty}\frac{1}{2^u u!}(kz)^{u+1} H_{u-1}^1(kz) b^{2u}, \tag{21}$$

where H^1_{u-1} is the $(u-1)$th-order spherical Bessel function of the third kind. Eq. (20) can be expressed as

$$\begin{aligned} E_x(\rho,z,\theta) &= \frac{1}{f^2}\exp(im\theta)\sum_{u=0}^{\infty}\sum_{l=0}^{n}\sum_{s=0}^{l}\frac{(-1)^{l+s}}{2^{u+2s+m+1}u!s!}\binom{n+m}{n-l} \\ &\quad \binom{l+m}{l-s}(kz)^{u+1}H^1_{u-1}(kz) \\ &\quad \left(\int_0^\infty - \int_1^\infty\right)\frac{b^{2s+m+2u}}{f^{2s+m}}\exp\left(-\frac{b^2}{4f^2}\right)J_m(kb\rho)bdb. \end{aligned} \tag{22}$$

When $1/f^2$ is large, the second integral term in Eq. (22) is controlled by the Gaussian exponential term. With the fixed values of n and m, the second integral can be neglected for the certain range of f, which has been demonstrated in Refs. [35–38]. When $n = m = 0$, the omission of the second integral is allowed for the case of $f \leq 0.2$. When $n + m/2 \leq 15$, the omission of the second integral is allowed for the case of $f \leq 0.055$ [39]. When the second integral is omitted, Eq. (22) analytically turns out to be

$$\begin{aligned} E_x(\rho,z,\theta) = &\left(\frac{\rho}{w_0}\right)^m \exp\left(-\frac{\rho^2}{w_0^2}\right)\exp(im\theta)\sum_{u=0}^{\infty}\sum_{l=0}^{n}\sum_{s=0}^{l}(-1)^{l+s}2^u f^{2u} \\ &\binom{n+m}{n-l}\binom{l+m}{l-s}\binom{u+s}{u} \\ &(kz)^{u+1}H^1_{u-1}(kz)L^m_{s+u}\left(\frac{\rho^2}{w_0^2}\right). \end{aligned} \tag{23}$$

When u only takes 0, Eq. (23) is just the paraxial solution. Therefore, our result includes numerous correction terms, which is characterized by f^{2u} $(u \neq 0)$. Therefore, here the procedure is performed beyond the paraxial approximation. The longitudinal component of the optical field of the elegant Laguerre-Gaussian beam reads as

$$\begin{aligned} E_z(\rho,z,\theta) &= -\frac{i\cos\theta}{2f^2}\exp(im\theta)\sum_{l=0}^{n}\sum_{s=0}^{l}\frac{(-1)^{l+s}}{2^{2s+m}s!}\binom{n+m}{n-l}\binom{l+m}{l-s} \\ &\quad \int_0^\infty \frac{b^{2s+m}}{f^{2s+m}}\exp\left(-\frac{b^2}{4f^2}\right)J_{m+1}(k\rho b)\frac{\exp(ik\gamma z)}{\gamma}b^2db. \end{aligned} \tag{24}$$

When $b < 1$, the following expansion is valid [34]

$$\frac{\exp(ik\gamma z)}{\gamma} = \sum_{u=0}^{\infty}\frac{i}{2^u u!}(kz)^{u+1}H^1_u(kz)b^{2u}. \tag{25}$$

Similarly, the longitudinal component of the optical field of the elegant Laguerre-Gaussian beam can be analytically expressed as

$$E_z(\rho,z,\theta)=\frac{1}{2}\left(\frac{\rho}{w_0}\right)^{m+1}\exp\left(-\frac{\rho^2}{w_0^2}\right)\{\exp[i(m+1)\theta]-\exp[i(m-1)\theta]\}$$
$$\sum_{u=0}^{\infty}\sum_{l=0}^{n}\sum_{s=0}^{l}2^{u+1}(-1)^{l+s}f^{2u+1}\left(\begin{array}{c}n+m\\n-l\end{array}\right)$$
$$\left(\begin{array}{c}l+m\\l-s\end{array}\right)\left(\begin{array}{c}u+s\\u\end{array}\right)(kz)^{u+1}H_u^1(kz)L_{u+s}^{m+1}\left(\frac{\rho^2}{w_0^2}\right). \quad (26)$$

As the orbital angular momentum density involves the Poyting vector, the definition of the Poyting vector is based on the electric and the magnetic fields. By taking the curl of the electric field, the magnetic field of the elegant Laguerre-Gaussian beam turns out to be

$$\mathbf{H}(\rho,z,\theta)=\frac{i}{\omega\mu_0}\nabla\times\mathbf{E}(\rho,z,\theta), \quad (27)$$

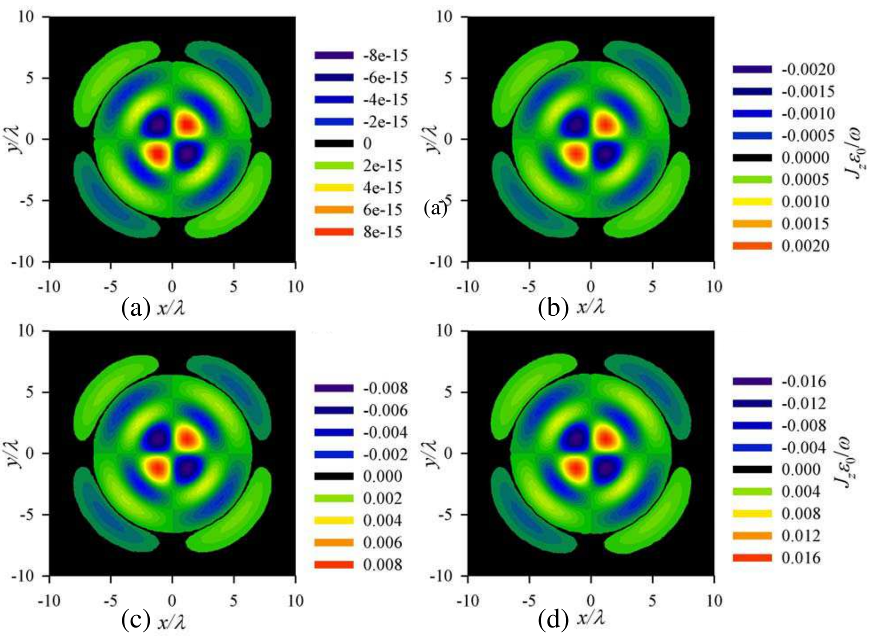

Figure 1. The orbital angular momentum density of the elegant Laguerre-Gaussian beam in different reference planes. $w_0 = 5\lambda$, $n = 3$, and $m = 0$. (a) $z = 0$. (b) $z = 5\lambda$. (c) $z = 10\lambda$. (d) $z = 15\lambda$.

where μ_0 is the magnetic permeability of vacuum. Eq. (27) is just one of Maxwell's equations, which is the exact solution. As no paraxial approximation is used, the electromagnetic fields of the elegant Laguerre-Gaussian beam propagating in free space are derived beyond the paraxial approximation. For the certain range of f, the omission in the electric field does not affect the magnetic field, which can be verified by the self-consistence of Maxwell's equation:

$$\mathbf{E}(\rho, z, \theta) = -i\omega\varepsilon_0 \nabla \times \mathbf{H}(\rho, z, \theta), \tag{28}$$

where ε_0 is the electric permittivity of vacuum. The Poyting vector of the elegant Laguerre-Gaussian beam is given by

$$\begin{aligned} \mathbf{S}(\rho, z, \theta) &= \frac{1}{4} \langle \mathbf{E}(\rho, z, \theta) \times \mathbf{H}^*(\rho, z, \theta) + \mathbf{E}^*(\rho, z, \theta) \times \mathbf{H}(\rho, z, \theta) \rangle \\ &= S_x(\rho, z, \theta)\mathbf{i} + S_y(\rho, z, \theta)\mathbf{j} + S_z(\rho, z, \theta)\mathbf{k}, \end{aligned} \tag{29}$$

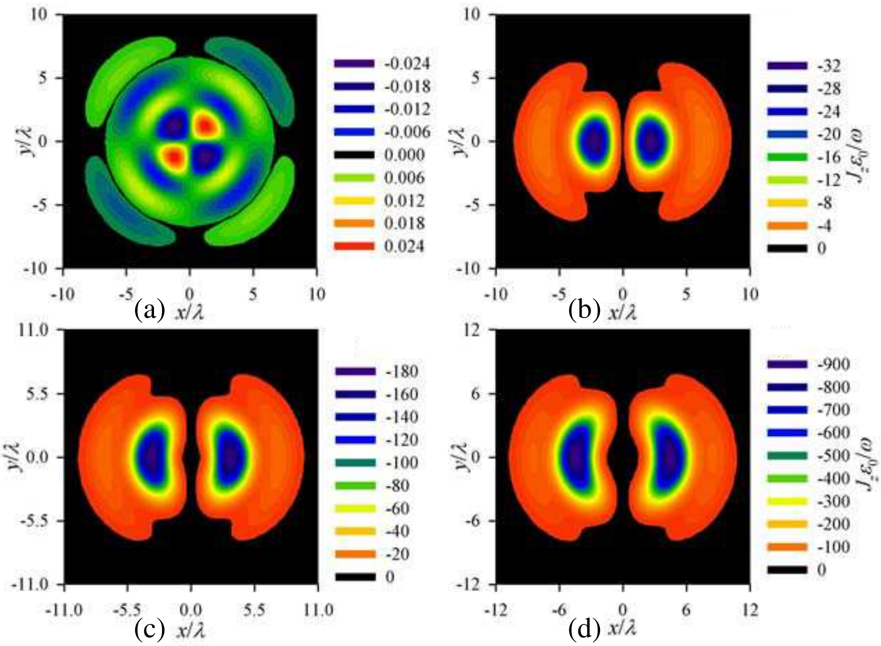

Figure 2. The orbital angular momentum density of the elegant Laguerre-Gaussian beam in the reference plane $z = 20\lambda$. $w_0 = 5\lambda$ and $n = 3$. (a) $m = 0$. (b) $m = 1$. (c) $m = 2$. (d) $m = 3$.

with $S_x(\rho,\ z,\ \theta)$, $S_y(\rho,\ z,\ \theta)$, and $S_z(\rho,\ z,\ \theta)$ being given by

$$\begin{aligned} S_x(\rho,z,\theta) &= \frac{i}{4\omega\mu_0}\left\{E_z(\rho,z,\theta)\left[\frac{\partial E_x^*(\rho,z,\theta)}{\partial z}-\frac{\partial E_z^*(\rho,z,\theta)}{\partial x}\right]\right. \\ &\quad \left.-E_z^*(\rho,z,\theta)\left[\frac{\partial E_x(\rho,z,\theta)}{\partial z}-\frac{\partial E_z(\rho,z,\theta)}{\partial x}\right]\right\}, \qquad (30) \\ S_y(\rho,z,\theta) &= \frac{i}{4\omega\mu_0}\left[E_x^*(\rho,z,\theta)\frac{\partial E_x(\rho,z,\theta)}{\partial y}-E_x(\rho,z,\theta)\frac{\partial E_x^*(\rho,z,\theta)}{\partial y}\right. \\ &\quad \left.+E_z^*(\rho,z,\theta)\frac{\partial E_z(\rho,z,\theta)}{\partial y}-E_z(\rho,z,\theta)\frac{\partial E_z^*(\rho,z,\theta)}{\partial y}\right], \qquad (31) \\ S_z(\rho,z,\theta) &= \frac{i}{4\omega\mu_0}\left\{E_x^*(\rho,z,\theta)\left[\frac{\partial E_x(\rho,z,\theta)}{\partial z}-\frac{\partial E_z(\rho,z,\theta)}{\partial x}\right]\right. \\ &\quad \left.-E_x(\rho,z,\theta)\left[\frac{\partial E_x^*(\rho,z,\theta)}{\partial z}-\frac{\partial E_z^*(\rho,z,\theta)}{\partial x}\right]\right\}, \qquad (32) \end{aligned}$$

where the angle brackets indicate an average with respect to the time, and the asterisk denotes the complex conjugation. $\mathbf{j}$ is the unit vectors in the y-direction. In Eqs. (30)–(32), $E_y(\rho,\ z,\ \theta) = 0$ is taken into account. The orbital angular momentum density is defined as [40, 41]

$$\mathbf{J}(\rho,z,\theta)=\varepsilon_0\mu_0[\mathbf{r}\times\mathbf{S}(\rho,z,\theta)], \qquad (33)$$

where $\mathbf{r} = x\mathbf{i} + y\mathbf{j} + z\mathbf{k}$. Therefore, the orbital angular momentum density of the elegant Laguerre-Gaussian beam is found to be

$$\mathbf{J}(\rho,z,\theta)=J_x(\rho,z,\theta)\mathbf{i}+J_y(\rho,z,\theta)\mathbf{j}+J_z(\rho,z,\theta)\mathbf{k}, \qquad (34)$$

with $J_x\ (\rho,\ z,\ \theta)$, $J_y\ (\rho,\ z,\theta)$, and $J_z\ (\rho,\ z,\ \theta)$ being given by

$$\begin{aligned} J_x(\rho,z,\theta) &= \varepsilon_0\mu_0[yS_z(\rho,z,\theta)-zS_y(\rho,z,\theta)], \qquad (35) \\ J_y(\rho,z,\theta) &= \varepsilon_0\mu_0[zS_x(\rho,z,\theta)-xS_z(\rho,z,\theta)], \qquad (36) \\ J_z(\rho,z,\theta) &= \varepsilon_0\mu_0[xS_y(\rho,z,\theta)-yS_x(\rho,z,\theta)], \qquad (37) \end{aligned}$$

Inserting Eqs. (23) and (26) into Eqs. (35)–(37), one can obtain the orbital angular momentum density of the elegant Laguerre-Gaussian beam. The overall transverse components of the orbital angular momentum can be verified to be zero. Therefore, here we only consider the longitudinal component of the orbital angular momentum density. In Refs. [40, 41], the electromagnetic fields are treated within the framework of the paraxial approximation. While in the present paper, the electromagnetic fields are obtained beyond the paraxial approximation, which is the difference between the present paper and Refs. [40, 41].

3. NUMERICAL CALCULATIONS AND ANALYSES

Figure 1 represents the orbital angular momentum density of the elegant Laguerre-Gaussian beam in different reference plane where $w_0 = 5\lambda$, $n = 3$, and $m = 0$. When $n + m/2 \leq 15$, the obtained formulae are valid for $w_0 > 2.89\lambda$. Note that $\frac{\partial E_x(\rho,z,\theta)}{\partial z}$ is emerged in the expression of the orbital angular momentum density, the optical field of the elegant Laguerre-Gaussian beam in the source plane is described by Eqs. (8) and (12). When $m = 0$, the areas of the positive and the negative angular momentum densities are symmetrical. The overall angular momentum in the reference plane is zero. The distribution of the positive angular momentum density is located along the $\pi/4$ line with respect to the x-axis, and the distribution of the negative angular momentum density is located along the $3\pi/4$ line with respect to the x-axis. Though the angular mode in the x-component of the elegant Laguerre-Gaussian beam is m, the angular mode in the longitudinal component of the elegant Laguerre-Gaussian beam is a mixed one of $m + 1$ and $m - 1$, which results in the above distribution. Upon propagation, the profile of the orbital angular momentum density

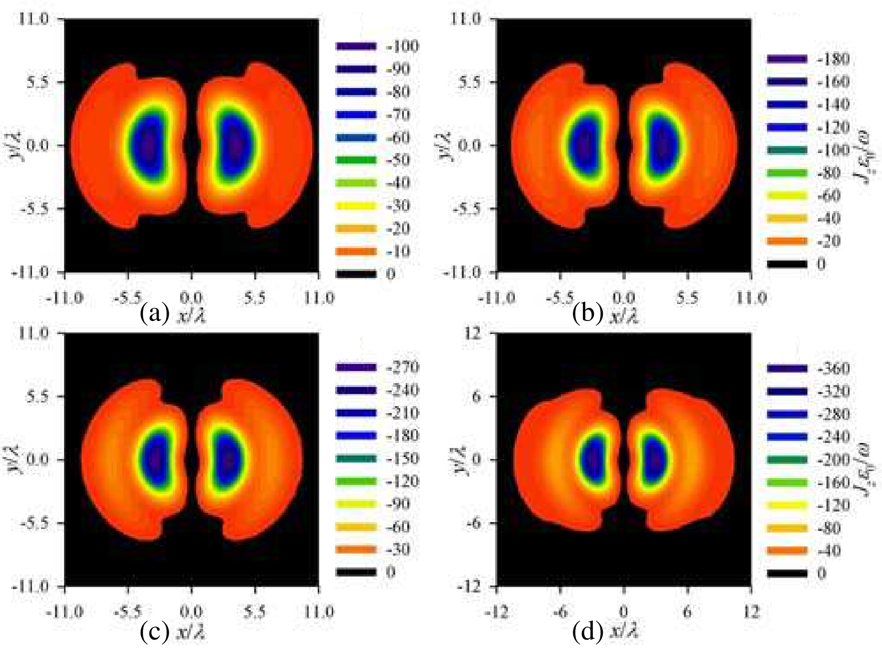

Figure 3. The orbital angular momentum density of the elegant Laguerre-Gaussian beam in the reference plane $z = 20\lambda$. $w_0 = 5\lambda$ and $m = 2$. (a) $n = 2$. (b) $n = 3$. (c) $n = 4$. (d) $n = 5$.

slowly expands, and the magnitude of the orbital angular momentum density increases.

The orbital angular momentum density of the elegant Laguerre-Gaussian beam in a reference plane is determined by the angular mode number, the radial mode number, and the beam waist width. Now, we investigate the effects of these three beam parameters on the distribution of the orbital angular momentum density, which are shown in Figs. 2–4. The reference plane is fixed to be $z = 20\lambda$. $w_0 = 5\lambda$ and $n = 3$ in Fig. 2. When m is a positive integer, the orbital angular momentum density is negative, which only indicates the spiral direction. The distribution of the orbital angular momentum density is composed of two symmetrical lobes, which are located in the horizontal direction. With increasing the angular mode number, the magnitude of the orbital angular momentum density increases rapidly, and the pattern size of the orbital angular momentum density also slowly augments. However, the shape of the distribution of the orbital angular momentum density does not change a lot. In Fig. 3, m is kept to be 2 and n varies. With increasing the radial mode number, the magnitude and the pattern size of the orbital angular momentum

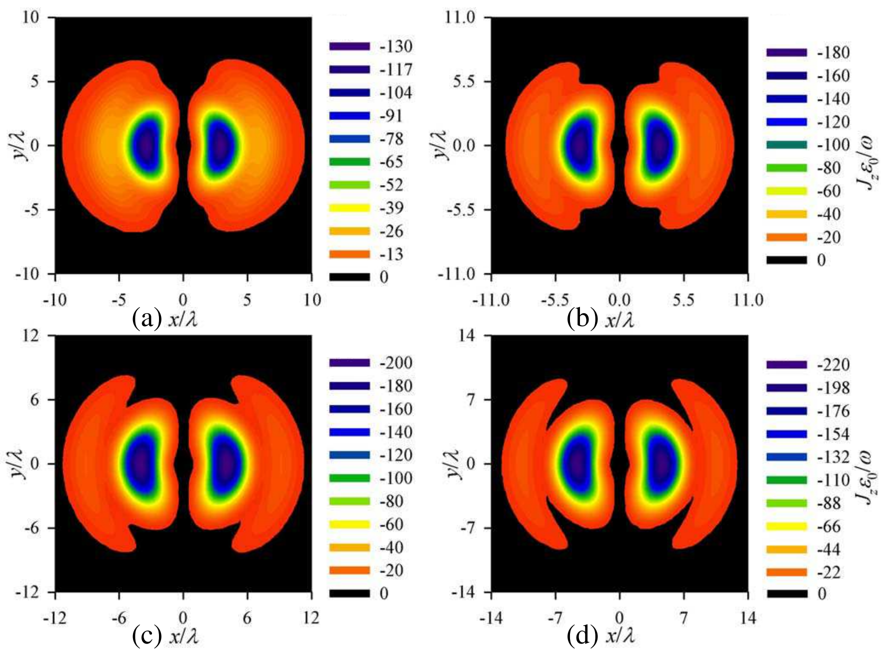

Figure 4. The orbital angular momentum density of the elegant Laguerre-Gaussian beam in the reference plane $z = 20\lambda$. $m = 2$ and $n = 3$. (a) $w_0 = 4\lambda$. (b) $w_0 = 5\lambda$. (c) $w_0 = 6\lambda$. (d) $w_0 = 7\lambda$.

density both increase. However, the orbital angular momentum density is more sensitive to the angular mode number than to the radial mode number. With increasing the radial mode number, the change in the shape of the distribution of the orbital angular momentum density is also little. In Fig. 4, $m = 2$, $n = 3$, and the beam waist width of the fundamental Gaussian mode is a variable. With increasing the beam waist width of the fundamental Gaussian mode, the magnitude and the pattern size of the orbital angular momentum density also increase. Nevertheless, the orbital angular momentum density is more sensitive to the radial mode number than to the beam waist width. Comparatively, the change in the shape of the distribution of the orbital angular momentum density is more noticeable with altering the beam waist width.

For the convenience of comparison, the distributions of the orbital angular momentum density of a standard Laguerre-Gaussian beam in the reference plane $z = 20\lambda$ are shown in Figs. 5–7. The equation used is from Ref. [39]. Figs. 5–7 match with Figs. 2–4 in terms of beam parameters. Under the same conditions, the distributions of the orbital

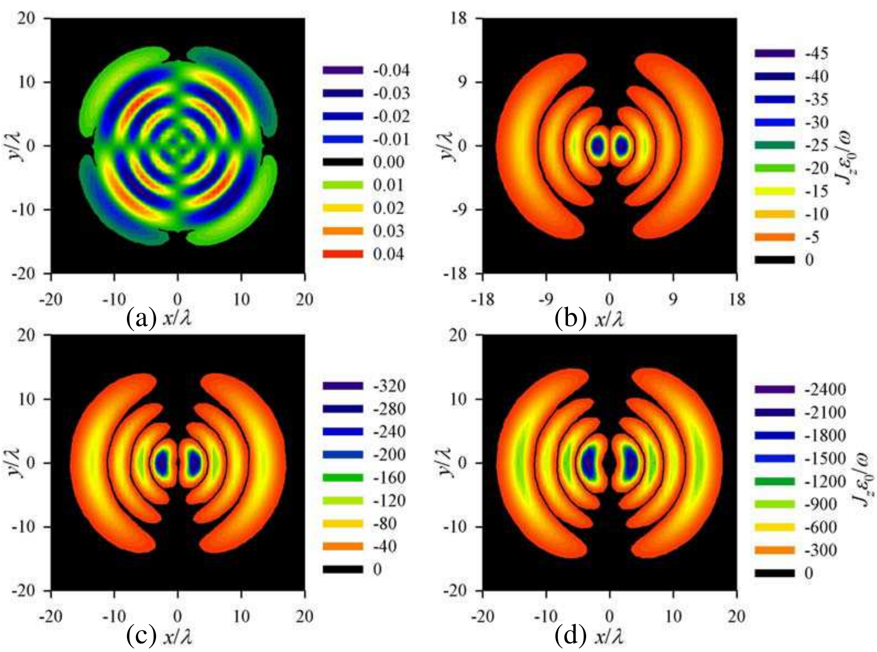

Figure 5. The orbital angular momentum density of the standard Laguerre-Gaussian beam in the reference plane $z = 20\lambda$. $w_0 = 5\lambda$ and $n = 3$. (a) $m = 0$. (b) $m = 1$. (c) $m = 2$. (d) $m = 3$.

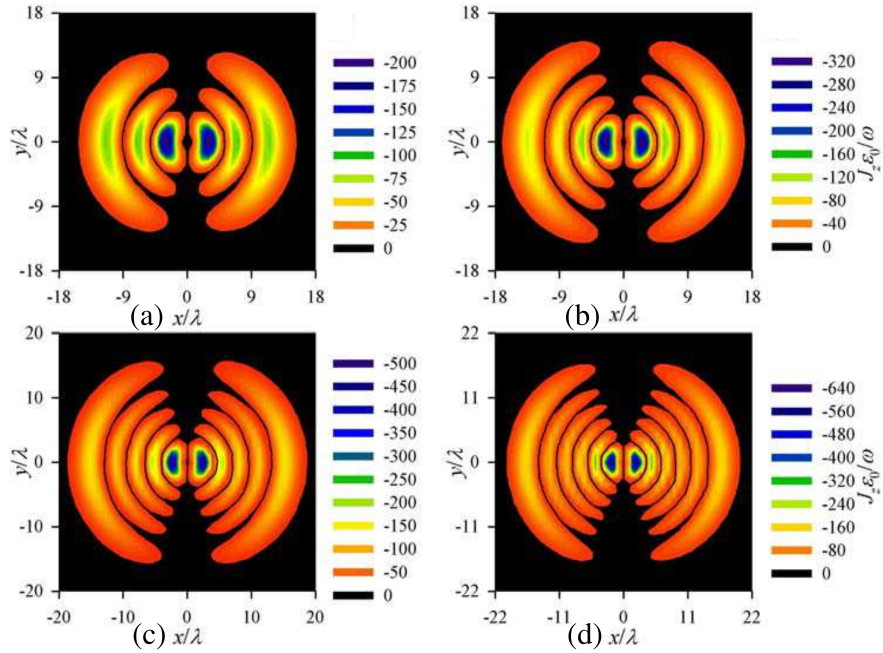

Figure 6. The orbital angular momentum density of the standard Laguerre-Gaussian beam in the reference plane $z = 20\lambda$. $w_0 = 5\lambda$ and $m = 2$. (a) $n = 2$. (b) $n = 3$. (c) $n = 4$. (d) $n = 5$.

angular momentum density of elegant and standard Laguerre-Gaussian beams are different. When $m = 0$, the positive and the negative angular momentum densities takes on staggered distribution. When m is a positive integer, the distribution of the orbital angular momentum density is composed of two central lobes and n pairs of side lobes, which surround the two central lobes. All of the lobes are located in the horizontal direction. With increasing the angular mode number or the beam waist width, the shape of the distribution of the orbital angular momentum density keeps nearly invariant and only expands in the pattern size. With increasing the radial mode number, the number of the side lobes surrounding the central lobes increases, and the pattern size also augments. Under the same conditions, the magnitude and the pattern size of the orbital angular momentum density of the standard Laguerre-Gaussian beam are both larger than those of the elegant Laguerre-Gaussian beam. However, elegant and standard Laguerre-Gaussian beams have one thing in common. Of the angular mode number, the radial mode number, and the beam waist width, the orbital angular momentum density is most sensitive to the angular

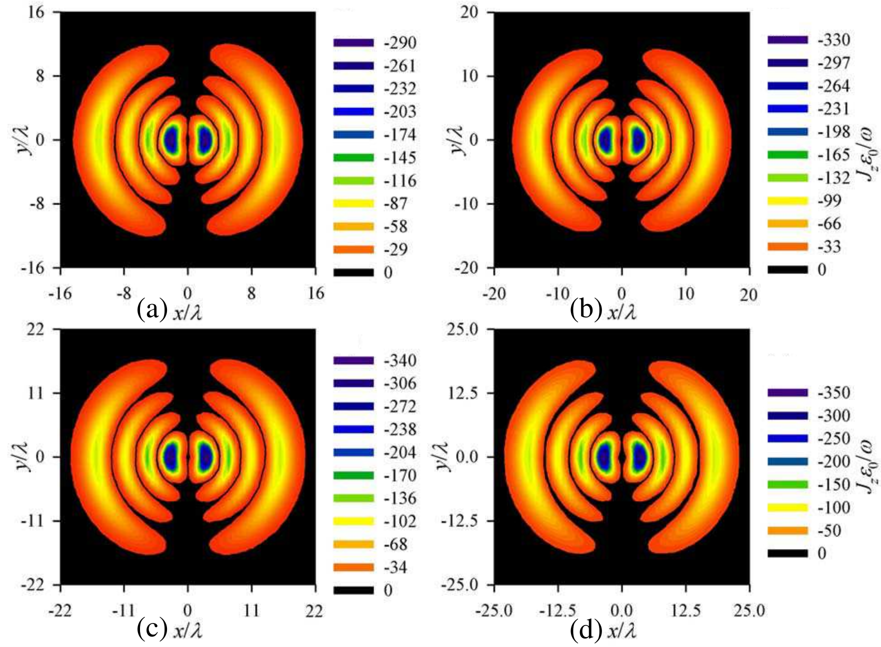

Figure 7. The orbital angular momentum density of the standard Laguerre-Gaussian beam in the reference plane $z = 20\lambda$. $m = 2$ and $n = 3$. (a) $w_0 = 4\lambda$. (b) $w_0 = 5\lambda$. (c) $w_0 = 6\lambda$. (d) $w_0 = 7\lambda$.

mode number and is most insensitive to the beam waist width. The advantage of the elegant Laguerre-Gaussian beam over the standard Laguerre-Gaussian beam is the relatively uniform distribution of the orbital angular momentum density.

4. CONCLUSIONS

Based on the method of the vectorial angular spectrum, an analytical expression of the electric field of the elegant Laguerre-Gaussian beam in free space is derived beyond the paraxial approximation. The magnetic field of the elegant Laguerre-Gaussian beam is given by taking the curl of the obtained electric field. By using the expressions of the electromagnetic fields for the elegant Laguerre-Gaussian beam, the expression of the orbital angular momentum density of the elegant Laguerre-Gaussian beam is derived. The formula is applicable to both the near and far fields. As the overall transverse component of the orbital angular momentum is zero, only the longitudinal component of the orbital angular momentum density is taken into account.

The effects of the three beam parameters on the distribution of the orbital angular momentum density of the elegant Laguerre-Gaussian beam are examined. When $m \neq 0$, the distribution of the orbital angular momentum density is relatively stable and is composed of two symmetrical lobes. To acquire the maximum orbital angular momentum density, the optimal choice is to increase the angular mode number, and the second best choice is to increase the radial mode number. Also, the distribution of the orbital angular momentum density of the elegant Laguerre-Gaussian beam is compared with that of the standard Laguerre-Gaussian beam. When $m \neq 0$, the distribution of the orbital angular momentum density of the standard Laguerre-Gaussian beam is composed of two central lobes and n pairs of side lobes. Under the same conditions, the magnitude and the pattern size of the orbital angular momentum density of the standard Laguerre-Gaussian beam are both larger than those of the elegant Laguerre-Gaussian beam. However, the distribution of the orbital angular momentum density of the elegant Laguerre-Gaussian beam is more simple and centralized than that of the standard Laguerre-Gaussian beam. When altering the radial mode number, the distribution of the orbital angular momentum density of the elegant Laguerre-Gaussian beam is more stable than that of the standard Laguerre-Gaussian beam. As mentioned in the optical field, one wants to know the distribution of the optical field. When mentioned in the orbital angular momentum, one also wants to know the distribution of the orbital angular momentum density. The distribution of the orbital angular momentum density is significant to the optical trapping, optical guiding, and optical manipulation. Therefore, the present study is useful to e.g. optical trapping, optical guiding, and optical manipulation with an elegant Laguerre-Gaussian beam.

ACKNOWLEDGMENT

This research was supported by National Natural Science Foundation of China under Grant Nos. 61178016, 10974179, and Zhejiang Provincial Natural Science Foundation of China under Grant No. Y1090073. The authors are indebted to Editorial Board Prof. Sailing He for useful discussions. Also, the authors are grateful to the reviewers for valuable comments.

REFERENCES

1. Takenaka, T., M. Yokota, and O. Fukumitsu, "Propagation of light beams beyond the paraxial approximate," *J. Opt. Soc. Am.*

A, Vol. 2, 826–829, 1985.

2. Zauderer, E., "Complex argument Hermite-Gaussian and Laguerre-Gaussian beams," *J. Opt. Soc. Am. A*, Vol. 3, 465–469, 1986.
3. Saghafi, S. and C. J. R. Sheppard, "Near field and far field of elegant Hermite-Gaussian and Laguerre-Gaussian modes," *J. Mod. Opt.*, Vol. 45, 1999–2009, 1998.
4. Deng, D., Q. Guo, L. Wu, and X. Yang, "Propagation of radially polarized elegant light beams," *J. Opt. Soc. Am. B*, Vol. 24, 636–643, 2007.
5. Luo, S. and B. Lü, "Propagation of the kurtosis parameter of elegant Hermite-Gaussian and Laguerre-Gaussian beams passing through *ABCD* systems," *Optik*, Vol. 113, 227–231, 2002.
6. Mei, Z. and D. Zhao, "Propagation of Laguerre-Gaussian and elegant Laguerre-Gaussian beams in apertured fractional Hankel transform systems," *J. Opt. Soc. Am. A*, Vol. 21, 2375–2381, 2004.
7. Mei, Z., "The elliptical elegant Laguerre-Gaussian beam and its propagation through aligned and misaligned paraxial optical systems," *Optik*, Vol. 118, 361–366, 2007.
8. Nasalski, W., "Elegant Hermite and Laguerre-Gaussian beams at a dielectric interface," *Opt. Appl.*, Vol. XL, 615–622, 2010.
9. Qu, J., Y. Zhong, Z. Cui, and Y. Cai, "Elegant Laguerre-Gaussian beam in a turbulent atmosphere," *Opt. Commun.*, Vol. 283, No. 14, 2772–2781, 2010.
10. Xu, H., Z. Cui, and J. Qu, "Propagation of elegant Laguerre-Gaussian beam in non-Kolmogorov turbulence," *Opt. Express*, Vol. 19, 21163–21173, 2011.
11. Chu, X., "Evolution of elegant Laguerre-Gaussian beam disturbed by an opaque obstacle," *Journal of Electromagnetic Waves and Applications*, Vol. 26, No. 13, 1749–1755, 2012.
12. Ni, Y. and G. Zhou, "Nonparaxial propagation of an elegant Laguerre-Gaussian beam orthogonal to the optical axis of a uniaxial crystal," *Opt. Express*, Vol. 20, 17160–17173, 2012.
13. Zhao, D., Z. Mei, J. Gu, H. Mao, L. Chen, and S. Wang, "Propagation characteristics of truncated standard and elegant Laguerre-Gaussian beams," *Proc. SPIE*, Vol. 5639, 149–158, 2004.
14. Mei, Z. and D. Zhao, "The generalized beam propagation factor of truncated standard and elegant Laguerre-Gaussian beams," *J. Opt. A: Pure and Appl. Opt.*, Vol. 6, 1005–1011, 2004.
15. Zhou, G., "Vectorial structure of an elegant Laguerre-Gaussian beam in the far-field regime," *Lasers in Eng.*, Vol. 24, 127–146,

2012.

16. Bandres, M. A. and J. C. Gutiérrez-Vega, "Higher-order complex source for elegant Laguerre-Gaussian waves," *Opt. Lett.*, Vol. 29, 2213–2215, 2004.
17. Porras, M. A., R. Borghi, and M. Santarsiero, "Relationship between elegant Laguerre-Gauss and Bessel-Gauss beams," *J. Opt. Soc. Am. A*, Vol. 18, 177–184, 2001.
18. Pagani, Y. and W. Nasalski, "Diagonal relations between elegant Hermite-Gaussian and Laguerre-Gaussian beam fields," *Opto-Electron. Rev.*, Vol. 13, 51–60, 2005.
19. Gutiérrez-Vega, J. C., "Fractionalization of optical beams: II. Elegant Laguerre-Gaussian modes," *Opt. Express*, Vol. 15, 6300–6313, 2007.
20. Borghi, R., "Elegant Laguerre-Gauss beams as a new tool for describing axisymmetric flattened Gaussian beams," *J. Opt. Soc. Am. A*, Vol. 18, 1627–1633, 2001.
21. April, A., "Nonparaxial elegant Laguerre-Gaussian beams," *Opt. Lett.*, Vol. 33, 1392–1394, 2008.
22. Mei, Z. and J. Gu, "Comparative studies of paraxial and nonparaxial vectorial elegant Laguerre-Gaussian beams," *Opt. Express*, Vol. 17, 14865–14871, 2009.
23. Wang, F., Y. Cai, and O. Korotkova, "Partially coherent standard and elegant Laguerre-Gaussian beams of all orders," *Opt. Express*, Vol. 17, 22366–22379, 2009.
24. Wang, F., Y. Cai, H. T. Eyyuboglu, and Y. K. Baykal, "Average intensity and spreading of partially coherent standard and elegant Laguerre-Gaussian beams in turbulent atmosphere," *Progress In Electromagnetics Research*, Vol. 103, 33–56, 2010.
25. Luo, H., H. Xu, Z. Cui, and J. Qu, "Beam propagation factor of partially coherent Laguerre-Gaussian beams in non-Kolmogorov turbulence," *Progress In Electromagnetics Research M*, Vol. 22, 205–218, 2012.
26. He, H., M. E. Friese, N. R. Heckenberg, and H. Rubinsztein-Dunlop, "Direct observation of transfer of angular momentum to absorptive particles from a laser beam with a phase singularity," *Phys. Rev. Lett.*, Vol. 75, 826–829, 1995.
27. Curtis, J. E., B. A. Koss, and D. G. Grier, "Dynamic holographic optical tweezers," *Opt. Commun.*, Vol. 207, 169–175, 2002.
28. Gibson, G., J. Courtial, M. Padgett, M. Vasnetsov, V. Pas'ko, S. Barnett, and S. Franke-Arnold, "Free-space information transfer using light beams carrying orbital angular momentum,"

Opt. Express, Vol. 12, 5448–5456, 2004.

29. Lee, W. M., X.-C. Yuan, and W. C. Cheong, "Optical vortex beam shaping by use of highly efficient irregular spiral phase plates for optical micromanipulation," *Opt. Lett.*, Vol. 29, 1796–1798, 2004.
30. Paterson, C., "Atmospheric turbulence and orbital angular momentum of single photons for optical communication," *Phys. Rev. Lett.*, Vol. 94, 153901, 2005.
31. Li, C. F., "Spin and orbital angular momentum of a class of nonparaxial light beams having a globally defined polarization," *Phys. Rev. A*, Vol. 80, 063814, 2009.
32. Bliokh, K. Y., M. A. Alonso, E. A. Ostrovskaya, and A. Aiello, "Angular momentum and spin-orbit interaction of nonparaxial light in free space," *Phys. Rev. A*, Vol. 82, 063825, 2010.
33. Porras, M. A., "Nonparaxial vectorial moment theory of light beam propagation," *Opt. Commun.*, Vol. 127, 79–95, 1996.
34. Gradshteyn, I. S. and I. M. Ryzhik, *Table of Integrals, Series, and Products*, Academic Press, New York, 1980.
35. Agrawal, G. P. and D. N. Pattanayak, "Gaussian beam propagation beyond the paraxial approximation," *J. Opt. Soc. Am.*, Vol. 69, 575–578, 1979.
36. Cicchitelli, L., H. Hora, and R. Postle, "Longitudinal field components for laser beams in vacuum," *Phys. Rev. A*, Vol. 41, 3727–3732, 1990.
37. Chen, C. G., P. T. Konkola, J. Ferrera, R. K. Heilmann, and M. L. Schattenburg, "Analyses of vector Gaussian beam propagation and the validity of paraxial and spherical approximations," *J. Opt. Soc. Am. A*, Vol. 19, 404–412, 2002.
38. Cerjan, A. and C. Cerjan, "Analytica solution of flat-top Gaussian and Laguerre-Gaussian laser field components," *Opt. Lett.*, Vol. 35, 3465–3467, 2010.
39. Cerjan, A. and C. Cerjan, "Orbital angular momentum of Laguerre-Gaussian beams beyond the paraxial approximation," *J. Opt. Soc. Am. A*, Vol. 28, 2253–2260, 2011.
40. Gao, C., G. Wei, and H. Weber, "Orbital angular momentum of the laser beam and the second order intensity moments," *Science in China (Ser. A)*, Vol. 43, 1306–1311, 2000.
41. Allen, L., M. W. Beijersbergen, R. J. C. Spreeuw, and J. P. Woerdman, "Orbital angular momentum of light and the transformation of Laguerre-Gaussian laser modes," *Phys. Rev. A*, Vol. 45, 8185–8189, 1992.